CRAFT: A Tendon-Driven Hand with Hybrid Hard-Soft Compliance

Leo Lin*[1] Shivansh Patel*[1] Jay Moon*[1] Svetlana Lazebnik†[1] Unnat Jain†[2]

[1]University of Illinois Urbana-Champaign [2]UC Irvine

*Equal contribution †Equal advising

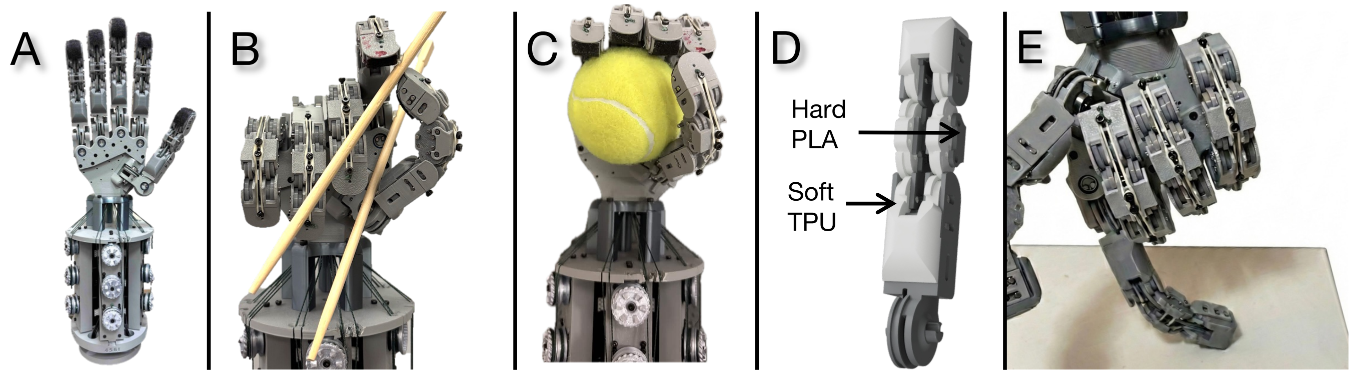

Fig. 1: **CRAFT Hand.** A) Full hand view showing the compact, anthropomorphic form factor with forearm-mounted actuators. B) CRAFT holding chopsticks to show complex dexterity. C) CRAFT holding a tennis ball, demonstrating its human-like size. D) One finger composed of hard PLA links and soft TPU joints. E) CRAFT conforming to a surface under contact, illustrating passive compliance at the joints.

***Abstract*—We introduce CRAFT hand, a tendon-driven anthropomorphic hand with hybrid hard-soft compliance for contact-rich manipulation. The design is based on a simple idea: contact is not uniform across the hand. Impacts concentrate at joints, while links carry most of the load. CRAFT places soft material at joints and keeps links rigid, and uses rolling-contact joint surfaces to keep flexion on repeatable motion paths. Fifteen motors mounted on the fingers drive the hand through tendons, keeping the form factor compact and the fingers light. In structural tests, CRAFT improves strength and endurance while maintaining comparable repeatability. In teleoperation, CRAFT improves handling of fragile and low-friction items, and the hand covers 33/33 grasps in the Feix taxonomy. The full design costs under $600 and will be released open-source with vision-based teleoperation and simulation integration. Project page: http://craft-hand.github.io/**

I. Introduction

Rigid, direct-drive robotic hands offer precise kinematics but are highly vulnerable to contact-rich impacts, which frequently interrupt data collection [25]. Conversely, soft robotic hands provide passive compliance to safely absorb collisions [7, 13, 17, 18], but suffer from low load capacities and unrepeatable, configuration-dependent kinematics. These failure modes stem from uniform material choices. Because manipulation impacts concentrate at joints while intermediate segments transmit actuation forces, we propose a hybrid style of compliance: *place compliant materials at joints to absorb shocks and use rigid links to maintain geometric predictability*.

To this end, we introduce the CRAFT hand (Fig. 1), a 3D-printed, 800g anthropomorphic platform costing under $600. It uses rigid polylactic acid (PLA) links for structural load paths and soft thermoplastic polyurethane (TPU) joints for impact absorption. Introducing soft joints historically raises two challenges: unrepeatable posture under load and structural fatigue. We resolve these by introducing: (1) a bidirectional mechanical linkage coupling the PIP and DIP joints for repeatable, load-independent postures, and (2) rolling-contact joint interfaces that distribute bending loads along a curved surface to minimize TPU stress concentrations [1].

To maintain an anthropomorphic form factor and protect components from collisions, 15 motors are routed behind the wrist. This tendon-driven configuration provides mechanical advantage for high holding strength and keeps the fingers light for natural teleoperation. We pair the hardware with a single-RGB whole-body teleoperation pipeline [25].

We evaluate CRAFT across three key axes:

1) **Structural Performance**: Benchmarked against the rigid LEAP hand [25], CRAFT matches its payload strength, precision, and repeatability.
2) **Robust Manipulation**: Teleoperation across five diverse tasks shows that passive force regulation dramatically improves success rates with fragile and low-friction objects.
3) **General Dexterity**: We demonstrate complete kinematic versatility by successfully executing all 33/33 grasps in the Feix taxonomy [8].

In summary, our contributions are: (i) a low-cost, open-source hybrid hard-soft hand morphology; (ii) coupled rolling-contact joint mechanisms that balance compliance with predictability; (iii) structural benchmarking against a rigid baseline; and (iv) validation across fragile teleoperation tasks and the full Feix taxonomy.

II. Related Work

Direct-Drive Hands. Classical direct-drive hands utilize rigid linkages and joint-mounted motors for precise control [28, 3, 9, 4], but are often costly [9], kinematically restricted [28], or bulky [4]. Modern low-cost baselines like the LEAP Hand [25] and D'Manus [4] improve accessibility, yet remain structurally stiff. Because these platforms rely on active impedance control rather than passive compliance to manage interaction forces, state estimation errors easily cause high-force, destructive collisions. In contrast, CRAFT integrates a compliant hard-soft structure with a human-like profile.

Tendon-Driven Designs. Relocating actuators to the forearm via tendons enables compact form factors [23, 11, 12, 19, 14, 30, 6]. While complex systems like the Shadow Hand [23] mimic human kinematics, high costs limit their deployment in large-scale learning. Recent open-source initiatives democratize this morphology but simplify kinematics by omitting critical degrees of freedom, such as abduction/adduction (RUKA [30]) or active DIP control (ORCA [6]). Crucially, these systems remain rigid, transferring torque directly to stiff joints. Our hand introduces soft material compliance directly into a high-DoF, fully articulated tendon layout.

Compliance and Soft Robotics. Soft robots use elastomer flexures [15, 29, 7, 19, 17] to passively absorb collisions, though underactuation often restricts dexterity. High-DoF hybrid architectures like Leap V2 [24] successfully unify robustness and dexterity, but prioritize extensive joint allocation over an ultra-compact profile. In contrast, CRAFT achieves a streamlined, sub-$600 anthropomorphic form factor for tight workspaces. Additionally, our rolling-contact joints replace fracture-prone flexures, eliminating stress concentrations to enhance durability.

III. Kinematic Design

CRAFT Hand Structure. Fully articulated and anthropomorphic, CRAFT features a 95 mm palm and 103 mm fingers for a 198 mm total length, matching median human male dimensions [10]. The hand weighs 800g and employs 15 actuators housed entirely within the forearm to actuate 15 active and 5 passive degrees of freedom (DoF) (Fig. 3).

Finger and Joint Mechanisms. Finger segments use rigid PLA to wrap load paths, while the metacarpophalangeal (MCP), proximal interphalangeal (PIP), and distal interphalangeal (DIP) joints use soft TPU flexures to absorb impacts (Fig. 4). Each finger utilizes three actuators to drive: (i) coupled PIP/DIP flexion, (ii) MCP abduction/adduction, and (iii) MCP flexion/extension.

At the PIP/DIP joints, a single tendon (Fig. 4**A**) acts through a bidirectional TPU linkage (Fig. 4**B**) that mechanically couples the joints to ensure equal, simultaneous rotation under variable loads. To prevent the mechanical fractures common to standard soft pin or flexure joints [25, 30], CRAFT implements rolling-contact interfaces [1]. This geometry constrains joint motion along a predictable kinematic path while distributing

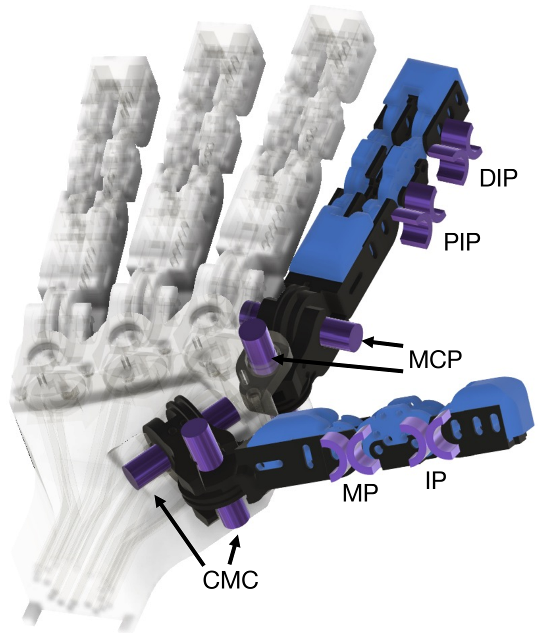

Fig. 3: **Joints Structure.** Black denotes the rigid components, while blue denotes the compliant (TPU) components. The index finger and thumb are highlighted to illustrate kinematics. The purple cylinders denote axes of rotation, while the purple half-circles denote the rolling-contact joints. Fingers feature a 2-DoF MCP and coupled PIP/DIP joints; the thumb mirrors this with a 2-DoF CMC and coupled MP/IP joints. PIP/DIP and MP/IP employ rolling contacts, while MCP/CMC use the cylindrical snap-fit interface.

stress across circular rolling profiles. Passive elastic bands (Fig. 4**C**) retract when tendon tension is relaxed.

At the MCP joint, backdrivable tendons (Fig. 4**D, E**) provide independent 2-DoF control, supported by a low-profile cylindrical snap-fit interface inspired by Christoph *et al.* [6]. This snap-fit architecture allows the joint to passively dislocate under extreme impacts rather than structurally failing. The thumb laterally mirrors this design exactly, utilizing a 2-DoF snap-fit carpometacarpal (CMC) joint and coupled rolling-contact joints for its intermediate phalanges.

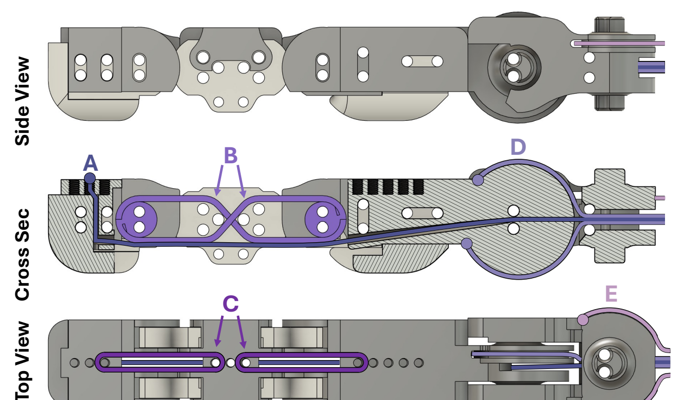

Fig. 4: **Finger Structure.** Dark gray denotes the hard (PLA) components and light gray denotes the soft (TPU) components. (A) PIP/DIP Tendon. (B) Bidirectional Linkage. (C) Elastic bands. (D) MCP Flexion/Extension Tendons. (E) Abduct/Adduct Tendons.

Tendon Routing Layout. High-strength braided lines route actuation forces from a pentagonal forearm motor assembly through smooth, internal metal dowels to minimize structural friction. Tendons are tensioned via ratchet spools [6].

IV. Experiments

We evaluate CRAFT along three axes. First, we test structural performance to measure the strength and precision that the hybrid design achieves relative to a rigid baseline. Second, we assess manipulation performance to determine whether passive compliance reduces operator effort and failures during teleoperation. Third, we validate grasp versatility to confirm that the hybrid design maintains the kinematic range and strength required for general manipulation.

A. Structural Tests

To evaluate the structural robustness of CRAFT hand, we conduct three assessments. We evaluate the strength, precision, and endurance of CRAFT to the LEAP hand [25] using standardized structural tests, consistent with prior work [30, 6]. It is a widely used rigid, direct-drive hand. To ensure a fair comparison, we assembled the LEAP hand using the same motors as CRAFT hand (Dynamixel XL330-M288-T instead of the $4\times$ expensive Dynamixel XC330-M288-T), hereafter denoted as `LEAP`. This allows us to make a head-on comparison between CRAFT and a rigid, direct-drive linkage (`LEAP`).

Pull-out Test (Strength). This experiment quantifies the maximum payload a finger can retain before mechanical failure. We command the finger to a fully flexed position and apply an external force opposing the flexion direction. The failure threshold is defined as the point where the finger slips or deflects by more than 15° from the target pose. We track the deflection angle using ArUco markers attached to the finger. As detailed in Tab. I, CRAFT withstands 15.29 N of pull-out force, nearly double the 8.67 N measured for the `LEAP` hand. This gap highlights the mechanical advantage of the tendon routing system. By distributing the load through the tendon, CRAFT reduces the direct torque demand on the motors compared to the direct-drive linkage of the `LEAP`, allowing for higher holding forces with identical actuation hardware.

Hand	CRAFT	`LEAP`
Visual	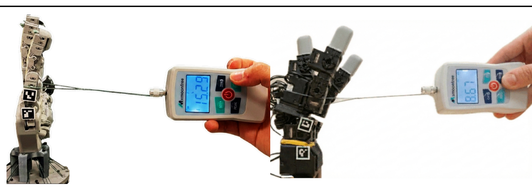	
Strength	15.29	8.67

TABLE I: **Pull-out Strength Comparison.** We measure the resistance of a flexed finger against an opposing external force (in N). The maximum force is recorded immediately prior to a fingertip deflection exceeding 15°. CRAFT demonstrates significantly higher retention strength due to the mechanical advantage of its tendon.

Repeatability Test (Precision). We investigate whether the tendon-driven mechanism introduces position errors or slack over prolonged operation. We program both hands to perform a grasp-and-release sequence on a plush toy continuously for one hour. Fig. 5 presents the joint angle tracking error over the duration of the experiment. The error is calculated using the motor encoder values. Both CRAFT and `LEAP` maintain consistent performance with mean tracking errors remaining below 0.01 rad. This result demonstrates that CRAFT achieves consistency similar to rigid hands, confirming that the benefits of compliance do not come at the cost of repeatability.

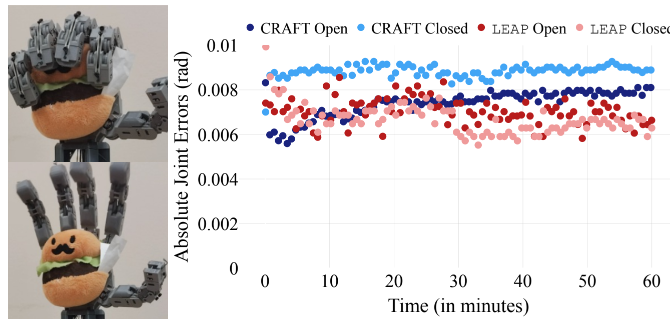

Fig. 5: **Repeatability under Cyclic Load.** *Left:* CRAFT performing continuous grasp-release cycles on an object. *Right:* Joint angle tracking error over one hour of operation. Despite the use of flexible tendons, CRAFT (blue dots) maintains a tracking error of < 0.01 rad, comparable to the rigid `LEAP` baseline (red dots), demonstrating consistent control. (shades depict joints closing and opening)

Holding Test (Endurance). Finally, we evaluate the hand's efficiency during high-load static holding. Both CRAFT and `LEAP` are commanded to grasp and hold a 5 lb dumbbell vertically for one hour (Fig. 6). We monitor the current draw to assess motor strain and thermal throttling. The results show that the average current consumption of CRAFT is approximately 50% lower than that of `LEAP`. While current draw in both hands rises initially as motor temperature increases, CRAFT stabilizes well below the motor's 600 mA limit. The friction inherent in the tendon routing acts as a passive braking mechanism, assisting in load retention and reducing the active torque required from the motors. In contrast, the direct-drive `LEAP` must constantly supply higher torque to combat the moment arm of the weight, leading to higher power consumption and thermal stress.

B. Teleoperation Tests and Simulation Model Verification

Teleoperation Evaluation Setup. To evaluate the real-world manipulation utility of CRAFT, we adapt the vision-based teleoperation framework of Sivakumar *et al.* [26] to drive the system (Fig. 7). An operator stands before a single markerless RGB camera (Fig. 7**A**), where FrankMocap [22] estimates 3D wrist trajectories (Fig. 7**B**) and HaMeR [20] tracks operator finger configurations (Fig. 7**C**). These tracked inputs map directly to the robot arm and CRAFT end-effector (Fig. 7**D**) using a joint-wise calibration procedure detailed in Appendix G. This unconstrained environment allows us to benchmark

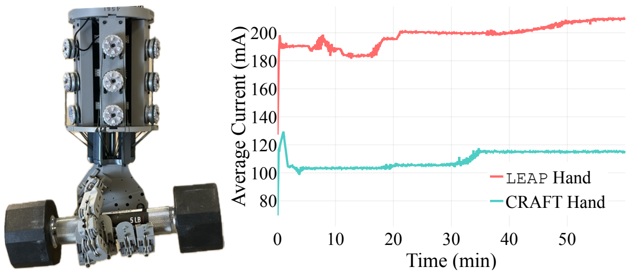

Fig. 6: **Holding Test**. We make CRAFT and LEAP hand grasp a heavy 5lb weight in its palm for one hour. On the vertical axis, we show that the average current running through CRAFT Hand is two times less compared to LEAP. The right axis shows that the current use initially increases. However, it still holds the weight and uses around one-third of its maximum possible current of 600mA.

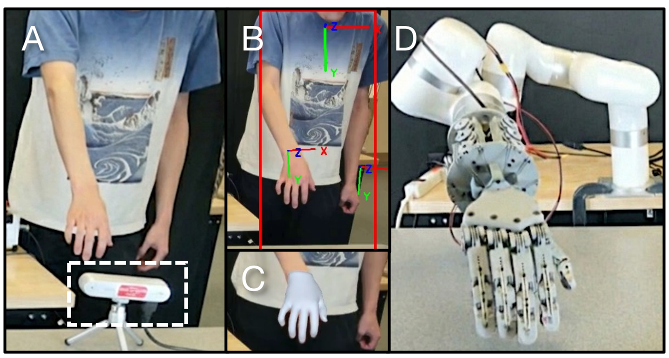

Fig. 7: **Whole-Arm Teleoperation.** **(A)** An operator stands in front of a single RGB camera (highlighted with a dashed box). **(B)** FrankMocap estimates the 3D pose of the operator's wrist relative to their torso, used for whole-arm retargeting. **(C)** HaMeR estimates the operator's hand pose for finger retargeting. **(D)** The estimated poses are mapped to CRAFT, mounted as the end-effector of a robotic arm.

hardware capabilities across open-world objects without the restrictions of data gloves or heavy sensors.

Teleoperation Tests. To evaluate real-world utility, we conduct a teleoperation user study comparing CRAFT against the rigid LEAP baseline across five distinct manipulation tasks that isolate specific contact challenges (e.g., fragility, scale, and low surface friction); detailed descriptions and photos of the test objects are provided in Appendix B.

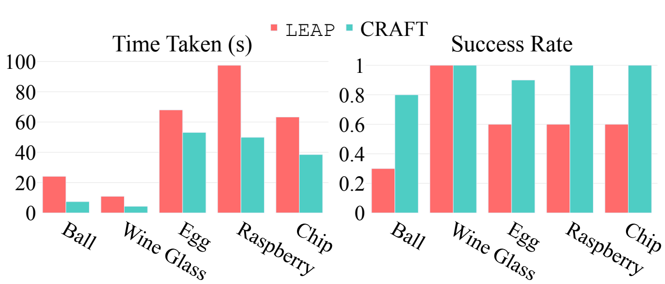

Fig. 8: **Teleoperation User Study Results.** Comparison of average completion time and success rate for five manipulation tasks. CRAFT consistently outperforms the LEAP hand, particularly in handling fragile objects (Raspberry, Chip) where compliance prevents damage, and in dynamic grasping (Ball) where adaptation simplifies capture.

C. Grasp Taxonomy Assessment

we evaluate CRAFT on the standardized Feix grasp taxonomy [8]. Driven by forearm-mounted tendon actuation, CRAFT covers all 33/33 distinct human grasp configurations ranging from power configurations to intricate precision pinches. A detailed qualitative breakdown and the full visual catalog of all 33 executed grasps are deferred to Appendix D.

D. Whole Arm Teleopration

To evaluate the practical utility of CRAFT across diverse manipulation scenarios, we demonstrate teleoperation on tasks shown in Fig. 9. Wiping a whiteboard with a sponge demonstrates the benefit of compliance during sustained surface contact, as the soft joints maintain consistent pressure. Twisting a key illustrates the advantage of compliance in contact-rich scenarios, where the joints absorb reaction forces during torque. Picking up a coin shows precision picking and compliance against obstacles. Picking up a raspberry tests precision grasping of small items, handling an egg requires managing low-friction fragility, and pouring from a wine glass validates stable manipulation of large breakable objects during dynamic motion. The hand completes all demonstrations without object damage or grasp failure, confirming that the hybrid design maintains functionality across a spectrum of functional tasks.

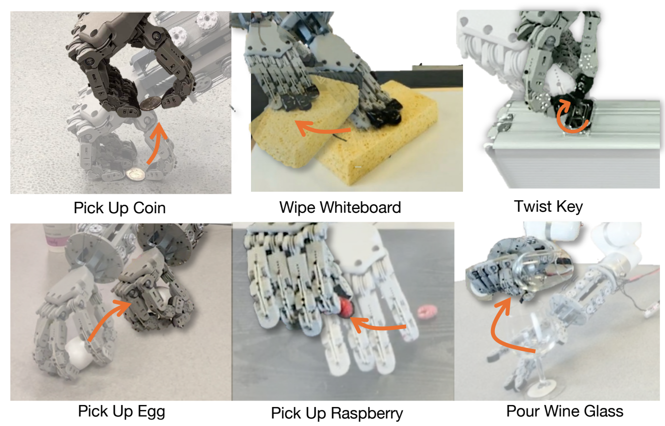

Fig. 9: **Whole Arm Teleoperation.** CRAFT executing various tasks, including wiping, picking fragile objects, and twisting a key.

E. Structural Comparison to Representative Robot Hands

Beyond rigid direct-drive systems, we compare CRAFT to representative anthropomorphic platforms (RUKA [30], ORCA [6], and Leap Hand V2 [24]) to evaluate kinematic range and profile constraints. A detailed breakdown of these structural trade-offs and physical workspace accessibility experiments can be found in Appendix C.

V. Conclusion

We introduce CRAFT, an open-source, hybrid hard-soft anthropomorphic hand designed for durable, data-driven dexterous learning. By localizing compliance at rolling-contact joints and rigidity at structural links, CRAFT matches the tracking precision of rigid baselines while doubling pull-out strength and reliably handling fragile items during teleoperation. Future work will leverage the hand's anthropomorphic profile to scale policy learning from human video demonstrations and simulation transfer.

VI. Acknowledgements

We thank the Siebel School Robotics Lab at UIUC and the School of Information and Computer Sciences at UC Irvine for their support. We are grateful to Akash Sharma, Kenneth Shaw, and Yuchen Song for feedback on the draft. We also thank Steven Oh and Kenneth Shaw for assistance with LEAP V2 demonstrations, as well as the members of UIUC SIGRobotics for helpful discussions. This work was supported in part by the 1517 Fund and Dynamixel.

References

[1] Jeongdo Ahn, Minho Hwang, Dukyoo Kong, Joonhwan Kim, and Dong-Soo Kwon. Asymmetric rolling contact joint for enhanced payload capabilities. *IEEE/ASME Transactions on Mechatronics*, 2023.

[2] Marcin Andrychowicz, Bowen Baker, Maciek Chociej, Rafal Jozefowicz, Bob McGrew, Jakub Pachocki, Arthur Petron, Matthias Plappert, Glenn Powell, Alex Ray, et al. Learning dexterous in-hand manipulation. *The International Journal of Robotics Research*, 2020.

[3] Barrett Technology. Barretthand. https://barrett.com/barretthand.

[4] Raunaq Bhirangi, Abigail DeFranco, Jacob Adkins, Carmel Majidi, Abhinav Gupta, Tess Hellebrekers, and Vikash Kumar. All the feels: A dexterous hand with large area sensing. *arXiv preprint arXiv:2210.15658*, 2022.

[5] Tao Chen, Megha Tippur, Siyang Wu, Vikash Kumar, Edward Adelson, and Pulkit Agrawal. Visual dexterity: In-hand reorientation of novel and complex object shapes. *Science Robotics*, 2023.

[6] Clemens C. Christoph, Maximilian Eberlein, Filippos Katsimalis, Arturo Roberti, Aristotelis Sympetheros, Michel R. Vogt, Davide Liconti, Chenyu Yang, Barnabas Gavin Cangan, Ronan J. Hinchet, and Robert K. Katzschmann. Orca: An open-source, reliable, cost-effective, anthropomorphic robotic hand for uninterrupted dexterous task learning. 2025. IROS 2025.

[7] Raphael Deimel and Oliver Brock. A novel type of compliant and underactuated robotic hand for dexterous grasping. *The International Journal of Robotics Research*, pages 161–185, 2016.

[8] Thomas Feix, Javier Romero, Heinz-Bodo Schmiedmayer, Aaron M Dollar, and Danica Kragic. The grasp taxonomy of human grasp types. *IEEE Transactions on human-machine systems*, 2015.

[9] German Aerospace Center (DLR). Dlr-hit hand ii. https://www.dlr.de/en/rm/research/robotic-systems/hands/dlr-hit-hand-ii. Accessed: 2025-12-24.

[10] Thomas M Greiner. Hand anthropometry of us army personnel. Technical report, 1991.

[11] Steve Jacobsen, Edwin Iversen, D Knutti, R Johnson, and K Biggers. Design of the utah/mit dextrous hand. In *Proceedings. 1986 IEEE International Conference on Robotics and Automation*. IEEE, 1986.

[12] Gaël Langevin. Inmoov hand. https://inmoov.fr/inmoov-hand/. Accessed: 2026-01.

[13] Haoran Li, Christopher J Ford, Matteo Bianchi, Manuel G Catalano, Efi Psomopoulou, and Nathan F Lepora. Brl/pisa/iit softhand: a low-cost, 3d-printed, underactuated, tendon-driven hand with soft and adaptive synergies. *IEEE Robotics and Automation Letters*, pages 8745–8751, 2022.

[14] Hong Liu, Ke Wu, Peter Meusel, Nikolaus Seitz, Gerd Hirzinger, MH Jin, YW Liu, SW Fan, T Lan, and ZP Chen. Multisensory five-finger dexterous hand: The dlr/hit hand ii. In *2008 IEEE/RSJ international conference on intelligent robots and systems*. IEEE.

[15] Raymond Ma and Aaron Dollar. Yale openhand project: Optimizing open-source hand designs for ease of fabrication and adoption. *IEEE Robotics & Automation Magazine*, 2017.

[16] Viktor Makoviychuk, Lukasz Wawrzyniak, Yunrong Guo, Michelle Lu, Kier Storey, Miles Macklin, David Hoeller, Nikita Rudin, Arthur Allshire, Ankur Handa, et al. Isaac gym: High performance gpu-based physics simulation for robot learning. *arXiv preprint arXiv:2108.10470*, 2021.

[17] Pragna Mannam, Kenneth Shaw, Dominik Bauer, Jean Oh, Deepak Pathak, and Nancy Pollard. A framework for designing anthropomorphic soft hands through interaction. *arXiv preprint arXiv:2306.04784*, 2023.

[18] Tad McGeer. Passive Dynamic Walking. *The International Journal of Robotics Research*, 9(2):62–82, 1990. doi: 10.1177/027836499000900206.

[19] Hyeonjun Park and Donghan Kim. An open-source anthropomorphic robot hand system: Hri hand. *HardwareX*, 2020.

[20] Georgios Pavlakos, Dandan Shan, Ilija Radosavovic, Angjoo Kanazawa, David Fouhey, and Jitendra Malik. Reconstructing hands in 3d with transformers. In *CVPR*, 2024.

[21] Haozhi Qi, Ashish Kumar, Roberto Calandra, Yi Ma, and Jitendra Malik. In-hand object rotation via rapid motor adaptation. In *Conference on Robot Learning*. PMLR, 2023.

[22] Yu Rong, Takaaki Shiratori, and Hanbyul Joo. Frankmocap: Fast monocular 3d hand and body motion capture by regression and integration. *arXiv preprint arXiv:2008.08324*, 2020.

[23] Shadow Robot Company. Shadow dexterous hand. https://www.shadowrobot.com.

[24] Kenneth Shaw and Deepak Pathak. Demonstrating leap hand v2: Low-cost, easy-to-assemble, high-performance hand for robot learning. *Robotics: Science and Systems (RSS)*, 2025.

[25] Kenneth Shaw, Ananye Agarwal, and Deepak Pathak.

Leap hand: Low-cost, efficient, and anthropomorphic hand for robot learning. *arXiv preprint arXiv:2309.06440*, 2023.

[26] Aravind Sivakumar, Kenneth Shaw, and Deepak Pathak. Robotic telekinesis: Learning a robotic hand imitator by watching humans on youtube, 2022. URL https://arxiv.org/abs/2202.10448.

[27] Emanuel Todorov, Tom Erez, and Yuval Tassa. Mujoco: A physics engine for model-based control. In *2012 IEEE/RSJ international conference on intelligent robots and systems*, 2012.

[28] Wonik Robotics. Allegro hand. https://www.wonikrobotics.com/research-robot-hand.

[29] Agisilaos G Zisimatos, Minas V Liarokapis, Christoforos I Mavrogiannis, George P Kontoudis, and Kostas J Kyriakopoulos. How to create affordable, modular, light-weight, underactuated, compliant robot hands. *National Technical University of Athens, Tech. Rep*, 2015.

[30] Anya Zorin, Irmak Guzey, Billy Yan, Aadhithya Iyer, Lisa Kondrich, Nikhil X. Bhattasali, and Lerrel Pinto. Ruka: Rethinking the design of humanoid hands with learning. *RSS*, 2025.

APPENDIX

A SIMULATION AND MODELING DETAILS

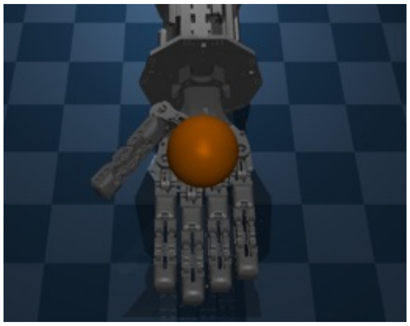

Fig. 10: **CRAFT in MuJoCo Simulation.** CRAFT grasping a sphere, with rolling contact joints modeled as equality constraints and joints treated as revolute constraints.

Simulation. For simulation-based policy learning, we provide URDF [16] and XML [27] files compatible with widely adopted simulators [2, 21, 5]. Currently, the URDF and MJCF models are primarily used to test out the mechanism and rolling contact joint in simulator. The simulation joint limits are set using range of motion measurements in real life and physical limits in the CAD design. Each actuated DoF is represented by a position actuator with joint limits matching the hardware's calibrated range.

B TELEOPERATION TEST

To validate whether CRAFT's compliance translates into improved utility in real-world manipulation, we conduct a teleoperation user study comparing CRAFT against the rigid LEAP baseline. We hypothesize that the passive compliance provided by the soft components will allow for higher success rates with fragile objects and faster completion times by reducing the cognitive load required for precise alignment. To test this, we experiment on five objects shown in Fig. 11, each selected to isolate a specific manipulation challenge:

1) **Grasping a Ball:** Requires no compliance, as the ball is solid. This is a reasonably easy object to grasp.
2) **Lifting a Wine Glass:** Requires handling a large, fragile object susceptible to shattering under excessive force.
3) **Handling an Egg:** Requires managing low-friction fragility, demanding a grasp that is delicate enough to prevent crushing but firm enough to prevent slip.
4) **Picking a Raspberry:** Requires extreme delicacy at a small scale, where the object is easily deformed by minor force.
5) **Lifting a Frito Chip:** Requires extreme delicacy, serving as a test for passive compliance.

To evaluate grasping performance in a controlled setting, we fixed the robot arm at an optimal pre-grasp pose for each task and allowed participants to control only the fingers via teleoperation. Before testing, participants were briefed on the mechanical differences between the two hands and given two minutes to familiarize themselves with the teleoperation interface. Each trial was limited to 150 seconds. We recruited 20 students and randomly assigned them to two non-overlapping groups of ten, with balanced robotics experience across groups. One group tested CRAFT, while the other tested the rigid baseline. Each participant completed five tasks in a fixed order, yielding 50 trials per hand and 100 in total.

Fig. 11: **Teleoperation User Study Objects.** To validate real-world utility, we evaluate teleoperation performance on five objects: (1) a ball (rigid grasping), (2) a wine glass (large and fragile), (3) an egg (low friction and fragile), (4) a raspberry (small and deformable), and (5) a frito chip (extremely delicate).

We measure both success rate and completion time across trials. Success rate captures whether the hand can complete the task at all, while completion time reflects the cognitive and control effort required from the operator. We plot the results in Fig. 8 and discuss them next.

We first examine the grasping ball task to test performance on rigid, non-deformable objects. The bulky structure of LEAP proved a confounding factor, making effective grasps difficult and resulting in taking a longer time and achieving a lower success rate. Since the ball is rigid, CRAFT's passive conformity played a minor role compared to other tasks.

Next, we evaluate lifting the wine glass to assess the manipulation of large, fragile objects. While the glass's substantial size made grasping it straightforward, the task highlighted a significant difference in user confidence. Those operating the rigid hand exhibited noticeable hesitation, moving slowly to avoid applying excessive force that might shatter the glass, taking more than twice as long to complete the task. Conversely, users with CRAFT leveraged the hand's passive compliance to close the grasp rapidly, trusting the soft hand to compensate for contact force. Since the glass's substantial size made grasping straightforward, both hands achieved a 100% success rate.

Handling the egg introduced the dual challenge of low surface friction and moderate fragility. The low friction proved to be the deciding factor, forcing LEAP users to operate with extreme caution and often taking significantly longer to attempt finding a stable grasp. CRAFT mitigated these risks through its compliant surface materials, which increased contact area, allowing users to secure the egg approximately 15 seconds faster on average than with the rigid hand. The rigid hand frequently failed to find a stable grasp before the time limit or slipped due to the lack of friction, resulting in a 60% success rate. CRAFT achieved a 90% success rate.

Finally, picking the raspberry and the chip were extreme delicacy tests of small objects, requiring precise force application. While users still required significant time (approx. 40-50 s) to carefully align the grasp for these small targets, the task exposed a critical difference in force regulation. The

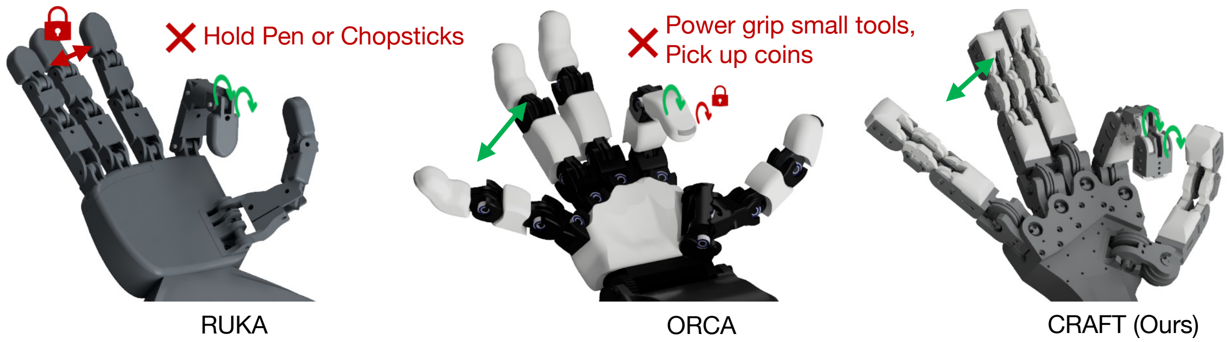

Fig. 12: **Finger Movement Comparison.** Unlike prior work, our hand incorporates both side-to-side movement from the base of the finger and active control of the first knuckle. In contrast, the RUKA hand [30] (RSS 2025) cannot move fingers sideways to squeeze objects, and the ORCA hand [6] (IROS 2025) lacks active control of the fingertips. By utilizing 20 degrees of freedom, our design enables significantly higher dexterity for tasks like picking up coins or using pens/chopsticks.

rigid hand frequently crushed objects upon contact due to the lack of passive give, resulting in a 60% success rate. CRAFT achieved a 100% success rate on both tasks, as the soft fingers absorbed contact forces. CRAFT's compliance became the deciding factor.

C Comparison to Representative Robot Hands

We compare the CRAFT design with representative anthropomorphic hands. While many other designs simplify kinematics to reduce complexity, CRAFT maintains full articulation within a compact form factor. We specifically contrast our kinematic structure with the RUKA and ORCA hands in Fig. 12, and evaluate our compact physical profile against the Leap Hand V2 in Fig. 13

RUKA [30]: The RUKA hand utilizes a simplified structure that omits abduction/adduction DoF. While this reduces mechanical complexity, it completely eliminates the lateral workspace of the fingers. This limitation prevents inter-finger grasps, such as holding objects between fingers, and does not allow the manipulation of tools like chopsticks or pens, which rely on lateral forces between fingers. The RUKA hand is unable to execute four Feix grasps due to this constraint, whereas CRAFT achieves full taxonomy coverage.

ORCA [6]: Similarly, the ORCA hand simplifies structure by employing a fixed DIP joint. This reduces the effective curling range of the fingers and limits the hand's ability to adjust the fingertips necessary for precise tasks. This, again, limits its ability to perform tasks such as holding chopsticks and a pen.

Leap V2 [24]: Leap V2 also adopts a hybrid hard-soft architecture but places some of its actuators behind the palm and fingers, resulting in a bulkier form factor than CRAFT. As demonstrated in Fig. 13, this limits its access in confined spaces: where Leap V2 collides with the environment, CRAFT's slim profile allows it to reach in.

D Grasp Taxonomy Validation Details

A crucial focus area in compliant robots is whether the introduction of compliance compromises the kinematic versatility required for general-purpose manipulation. To evaluate this, we assess CRAFT on the standardized benchmark of Grasp

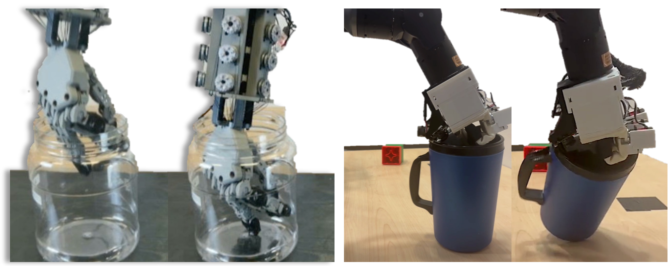

Fig. 13: **Narrow Space Accessibility.** CRAFT demonstrates the ability to fit into a narrow jar, while the bulkier Leap Hand V2 fails to enter the same workspace due to its rigid linkage size. Both cans have the same radius. Results reproduced with the help of the authors of Leap Hand V2 [24]; reproduced in two labs with different cans.

Taxonomy introduced by Feix et al. [8] and as attempted by previous works [30]. This taxonomy formalizes human grasp types into a classification system, organizing grasps based on contact type, opposition direction, and hand shape. Consistent with prior works on open, robot hands [30], we evaluate on this benchmark because it represents the widest possible range of practically useful grasps required for daily activities.

Fig. 14 reports CRAFT's performance on this standardized set of 33 grasp types, achieving 33/33 successes compared to RUKA's 29/33. Tendon-driven actuation provides the flexion torque to secure objects in power configurations, like the Large Diameter (row 1, col 1). Complementing this, soft material properties facilitate conformal contact for precision grasps, such as the Prismatic 2 Finger (row 2, col 2), stabilizing the hold through local deformation. We highlight performance on configurations typically challenging for compliant mechanisms. The Adduction Grip (row 4, col 5) demonstrates the index finger's ability to maintain lateral stiffness against the thumb's orthogonal force. Similarly, the Writing Tripod (row 4, col 2) shows distal links can maintain specific geometry without collapsing under contact pressure. Finally, the Extension Type (row 7, col 3) validates the hand's full range of motion, forming a stable, flat platform for supporting objects.

E Teleoperation

For a hand to be useful for robot learning, it must map reliably to both a human operator and a simulator. We address

Fig. 14: **Grasp Taxonomy Validation.** CRAFT demonstrating 33 distinct grasp types from the Feix taxonomy [8]. The hand successfully executes a wide range of configurations, including power grasps (e.g., Large Diameter), precision grasps (e.g., Prismatic Pinch), and intermediate poses, confirming that the compliant design maintains the kinematic versatility required for general-purpose manipulation.

this in two steps: first, a calibration procedure that aligns the operator's hand range to the robot's joint limits, and then integration with vision-based teleoperation for data collection and verify kinematics in simulation.

Teleoperation. To teleoperate the hand, we must know how many motor turns move each joint across its full range. Following [6], we employ a joint-wise calibration procedure to align each operator's movements with CRAFT hardware. We begin by manually moving each robot joint to its extremes to record its range. We then record the operator's biological limits using HaMeR [20] as they move their fingers through their full range of motion, covering both flexion/extension and abduction/adduction. During teleoperation, a linear function maps the operator's current joint position, normalized against their biological range, to the corresponding angle within the robot's calibrated limits, ensuring accurate retargeting across all degrees of freedom.

With calibration in place, we follow the vision-based teleoperation framework of Sivakumar *et al.* [26] to collect demonstration data. As shown in Fig. 7**A**, the operator stands in front of a single RGB camera. FrankMocap [22] estimates the 3D pose of the operator's wrist relative to their torso (Fig. 7**B**), which is mapped to the robot's workspace for whole-arm retargeting. Simultaneously, HaMeR estimates the operator's hand pose (Fig. 7**C**) for finger retargeting. An exponential moving average is applied to smooth targets and mitigate noise inherent to vision-based tracking. Together, these estimates drive CRAFT, mounted as the end-effector of a robotic arm (Fig. 7**D**), enabling simultaneous control of the arm and hand with no wrist-mounted sensors or gloves. We also provide calibrated MuJoCo simulation models (see Appendix A).